JOURNAL OF CATALYSIS **168,** 154–163 (1997)
ARTICLE NO. CA971620

Nature of the Active Phase of a Nickel Catalyst during the Partial Oxidation of Methane to Synthesis Gas

F. van Looij[1] and J. W. Geus

Department of Inorganic Chemistry, Debije Institute, Utrecht University, Sorbonnelaan 16, 3584 CA Utrecht, The Netherlands

Received November 10, 1995; revised January 6, 1997; accepted January 20, 1997

The study deals with the identification of the active nickel phase as a function of the oxygen conversion during the partial oxidation of methane to synthesis gas by means of *in situ* high-temperature X-ray diffraction (HTXRD), semi-*in situ* X-ray photoelectron spectroscopy (XPS) on a nonporous model catalyst (wafer), activity measurements, and temperature-programmed surface reaction (TPSR) experiments. The results demonstrate that the combustion of methane partly proceeds on bulk nickel oxide. A highly active phase, which is associated with partially oxidized nickel, is suggested to account for the major part of the combustion reaction. Finally, the reforming of methane to synthesis gas calls for the presence of metallic nickel sites. Evidently, the nature of the active phase is not uniform along the catalyst bed under reaction conditions. This highly complicating factor should be taken into account when investigating the mechanism of the partial oxidation of methane to synthesis gas. It is concluded that the results of mechanistic studies conducted at high oxygen conversion levels using either a fluidized bed reactor or a pulse apparatus should be considered with care.

INTRODUCTION

Additional hydrogen production capacity is presently required for sulfur removal from crude oil fractions such as gas oil (hydrotreating). The enhanced demand is due to the worldwide tightening of sulfur specifications and the simultaneously reduced hydrogen supply from catalytic reforming due to gasoline reformulation mandated by new laws (1–3). Moreover, hydrogen is needed for the production of ammonia and hydrogen peroxide (4). Synthesis gas is the feedstock for large-volume processes such as methanol and hydrocarbon synthesis (4, 5). Several routes exist for manufacturing synthesis gas from natural gas (2, 3, 6–10). The partial oxidation of methane is presently widely investigated for the production of synthesis gas (11).

The mechanism of the partial oxidation of methane to synthesis gas is still debated (12–29). Several studies suggest that the reaction mechanism involves the direct, selective oxidation of methane to both carbon monoxide and hydrogen. In contrast, other investigations state that methane is first converted with oxygen to carbon dioxide and water, followed by reforming of the remaining methane with carbon dioxide and water under the formation of synthesis gas. The reaction mechanism is closely related to the nature of the active site. Nevertheless, only little is known about the active phase during the partial oxidation of methane. Dissanayake *et al*. (21) first showed that the green catalyst layer on top of a black catalyst bed with an alumina-supported nickel catalyst can be attributed to the presence of nickel oxide (30) and metallic nickel, respectively. The aim of the present investigations was to identify the nature of both the surface layers and the bulk of the active nickel phase under reaction conditions. To that end, the current study employs a combination of *in situ* high-temperature X-ray diffraction (HTXRD), semi-*in situ* X-ray photoelectron spectroscopy (XPS) using a nonporous model catalyst with an infinitesimally low activity to assess the oxidation state of the surface layers of the nickel crystallites, activity measurements, and temperature-programmed surface reaction (TPSR) experiments.

The interaction of oxygen with nickel surfaces has been investigated extensively. The sticking probability is close to unity for Ni(100), Ni(111), and Ni(110) (31–36) at room temperature. The initial heat of adsorption of oxygen on nickel is high, viz., 500 kJ/mol (36–42). Oxide nucleation and lateral island growth on nickel films proceed once a critical oxygen surface coverage of 0.4 ML has been reached (32, 43, 44). Nickel readily forms three-dimensional oxides at high temperatures (31, 45, 46), while oxidation of metallic nickel at room temperature brings about the formation of a two-dimensional oxide with a thickness of two to three NiO layers (31, 33, 43). Phase transformations that readily proceed with oxygen as a single component may not occur in the presence of a reducing compound: the relative rates of the adsorption of oxygen and the reaction between oxygen and the compound to be oxidized govern the oxygen

[1] To whom correspondence should be addressed at the present address: Shell International Chemicals, Shell Research and Technology Centre Amsterdam (SRTCA), Department CTCAT/2, PO Box 38000, 1030 BN Amsterdam, The Netherlands.

0021-9517/97 $25.00

surface coverage θ_O at a given temperature and, hence, the nucleation of the oxidic phase. High oxygen-to-methane ratios can be expected to favor the formation of bulk nickel oxide, whereas complete oxidation of the nickel crystallites may be suppressed in the presence of an excess of the compound to be oxidized (46).

Recent investigations have shown (23, 25) that a huge temperature profile is present in the catalyst bed under steady-state conditions when undiluted methane/oxygen streams are used. To ensure isothermal operation, we employed diluted reactant mixtures in the present study. We demonstrate that the nature of the active phase significantly varies with the axial position in the catalyst bed. The consequences of this highly complicating factor for the mechanistic study of the partial oxidation of methane to synthesis gas using either a steady-state flow reactor or a pulse apparatus or a fluidized bed reactor are discussed.

METHODS

Catalysts

A 25 wt% nickel-on-silica catalyst was prepared by incipient wetness impregnation of silica (OX-50, Degussa, surface area 50 $m^2\ g^{-1}$) with a solution of nickel nitrate. Subsequent to drying, the catalyst was calcined in air at 720 K for 3 h. The mean nickel particle size was 30 nm, as deduced from hydrogen chemisorption experiments. The catalyst thus obtained is denoted as NL (large nickel crystallites).

A 25 wt% nickel-on-silica catalyst was prepared by homogeneous deposition–precipitation of nickel hydroxide onto silica (OX-50) by decomposition of urea at 363 K using a solution of nickel nitrate as a precursor (47). Subsequently, the loaded support was filtered, washed, and dried. The calcination of the catalyst was performed in air at 720 K for 3 h. Calculations from the extent of hydrogen chemisorption revealed that the mean nickel particle diameter was 6 nm. The catalyst thus obtained is denoted as NS (small nickel crystallites).

A model catalyst was prepared by spin-coating hydrated silicon wafers (48–50) employing a solution of 6 g $liter^{-1}$ nickel acetate in cyclohexanone. Subsequent to drying of the wafer at room temperature, calcination was performed in air at 730 K for 30 min. A reduced wafer was obtained by exposure of the sample to a stream of 70 ml(STP)/min hydrogen (99.9%) at 760 K for 30 min.

Catalytic Performance

Fifty milligrams of catalyst of a sieve fraction between 150 and 425 μm was placed into a quartz reactor of internal diameter 5.5 mm. Both above and below the catalyst bed 70 mg of silica (Aerosil 200, Degussa) of a sieve fraction between 500 and 850 μm was placed. Reduction of the calcined catalyst was performed in a flow of 10 vol% hydrogen (99.999%) in argon (99.999%) at 773 K for 3 h. The feed consisted of 1 vol% methane (99.998%) and 0.5 vol% oxygen (99.999%) in argon. All gases were provided by Hoek Loos B. V. and used without further purification. The total flow rate was 100 ml(STP)/min and as directed downstream. The product gases were analyzed with a mass spectrometer (Balzers QM420) every 30 s.

To measure the temperature, a chromel–alumel thermocouple was situated at the bottom of the catalyst bed. The temperature of the reactor was decreased from 900 to 520 K; at intervals of 15 K the temperature was kept constant for 20 min.

With a few experiments, a gas mixture containing 1 vol% methane and 0.5 vol% oxygen in argon was first combusted over 1 g of an alumina-supported manganese oxide catalyst (51) at 850 K. The gas mixture thus obtained consisted of methane, carbon dioxide, and water.

In Situ High-Temperature X-Ray Diffraction

Catalyst NL was ground and mixed with hexane. A thin layer of the obtained paste was applied onto a platinum grid. The sample was placed in a Guinier-Lenné X-ray diffractometer using Fe $K\alpha_{1,2}$ radiation ($\lambda = 1.93735$ Å) equipped with a high-temperature *in situ* chamber. The temperature of the chamber was raised in a flow of helium to 770 K. Subsequently, the catalyst was reduced in a flow of pure hydrogen for 4 h.

To establish the nickel oxidation state under various conditions, a part of a mixture of 2 vol% methane and 1 vol% oxygen in argon was first combusted over the manganese oxide catalyst at 850 K under the formation of a mixture of methane, carbon dioxide, and water in argon (25), while the remaining part of the gas stream bypassed the manganese oxide catalyst. The parallel gas streams thus obtained were mixed and subsequently fed to the *in situ* chamber of the diffractometer. The oxygen conversion level in the gas mixture could simply be adjusted by controlling the ratio of the parallel gas streams. The total flow rate was 100 ml/min. The catalyst was stabilized under the applied conditions at 825 K for at least 35 h before the X-ray diffraction pattern was recorded.

Semi-In Situ X-Ray Photoelectron Spectroscopy on a Model Catalyst

To reveal the nickel valence in the upper surface layers of the nickel crystallites under reaction conditions, a previously reduced $Ni/SiO_2/Si$ wafer was exposed to a flow containing methane, oxygen, carbon dioxide, and water in argon at 775 K for 16 h. The composition of the gas mixture, prepared as described above, corresponded to oxygen conversions of about 60 and 85%, respectively. Subsequent to evacuation, the sample was analyzed by means of XPS (Fisons).

Temperature-Programmed Surface Reaction by Methane

Two hundred fifty milligrams of a previously reduced catalyst was isothermally oxidized in a flow containing 2 vol% nitrous oxide (technical quality) in argon for 15 min. The reoxidation of the catalyst bed occurred under differential conditions. Consequently, the surface composition can be considered as being uniform along the catalyst bed. Subsequent to oxidation, the catalyst was quenched in argon to room temperature. The temperature of the catalyst bed fell below 320 K within 2 min. Temperature-programmed surface reaction was performed in a flow of 2 vol% methane in argon at a heating rate of 10 K/min.

RESULTS AND DISCUSSION

We investigated the influence of the nature of the nickel phase on both the level of conversion of methane and the composition of the product gas. Figure 1 shows the conversion of methane with oxygen at decreasing temperatures, employing either unreduced or freshly reduced catalyst NL. With the green nickel oxide catalyst the conversion of methane does not exceed a level of 25% at about 900 K, while carbon dioxide and water are the only products. With the previously reduced catalyst, on the other hand, the conversion of methane is well above 90% at 900 K, while synthesis gas is the main product. In addition, no synthesis gas was observed when a diluted mixture of methane, water vapor, and carbon dioxide was fed to the oxidic nickel catalyst. Large amounts of CO and H_2 were, on the other hand, found when a previously reduced catalyst was employed. The reforming of methane clearly calls for the presence of metallic nickel sites. That the nickel phase controls the activity of the catalyst for a given reaction path or a set of reactions is evident from both the oxidation and reforming experiments. Qualitatively the same results were obtained with catalyst NS, containing significantly smaller nickel crystallites than catalyst NL, viz., about 6 nm.

To identify the nature of the nickel phase as a function of the axial position in the catalyst bed, we stabilized a freshly reduced catalyst NL under reaction conditions for about 35 h at 825 K. Figure 2 shows the results of the subsequently conducted *in situ* HTXRD experiments. At low oxygen conversion levels, viz., 0 and 25%, only bulk nickel oxide is detected, confirming that the topmost green zone in the catalyst bed during the formation of synthesis gas (21) corresponds to the presence of bulk nickel oxide. The combined results of the *in situ* HTXRD and activity experiments suggest that the reoxidation of zero-valent nickel to bulk nickel oxide brings about the combustion of methane under oxygen-deficient conditions in the upper layers of

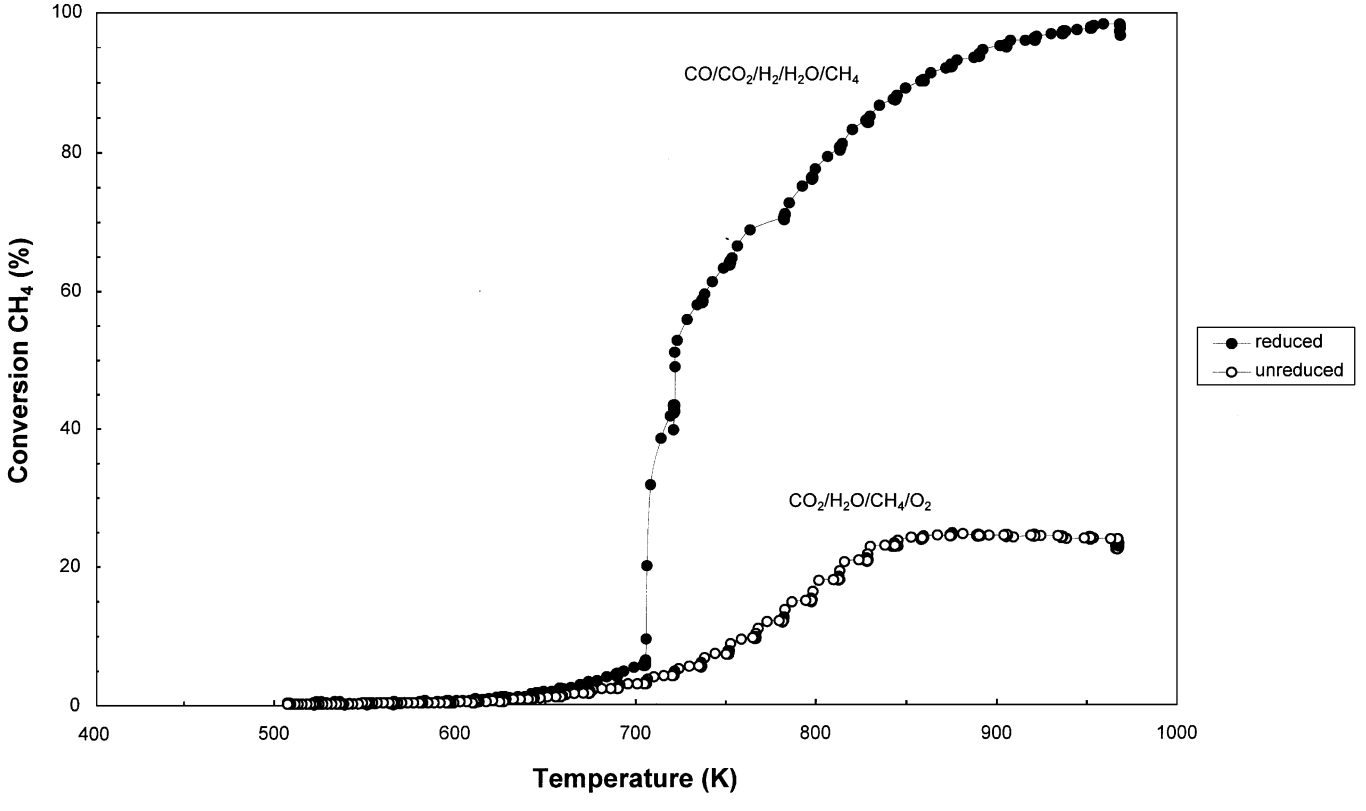

FIG. 1. Conversion of methane with oxygen employing either an unreduced or a reduced catalyst NL at decreasing temperatures. The reaction products are indicated in the figure.

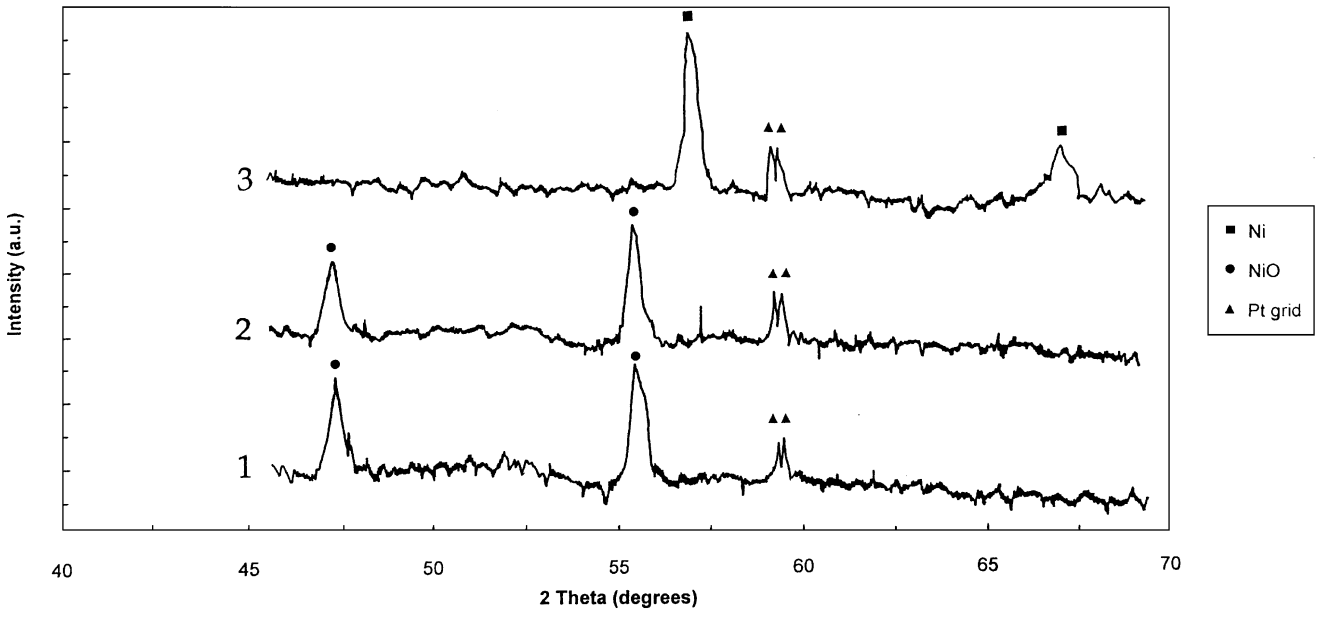

FIG. 2. *In situ* high-temperature X-ray diffraction patterns obtained subsequent to stabilization of the previously reduced nickel catalyst NL at 825 K under simulated reaction conditions corresponding to oxygen conversion levels of (1) 0%, (2) 25%, and (3) 60%. The peaks attributed to metallic platinum are due to the use of the platinum grid.

the catalyst bed. Interestingly, we previously observed that the selectivity toward synthesis gas dropped irreversibly to nil below a critical contact time (25). Since only the reduction of the catalyst could restore the high selectivity toward synthesis gas at longer contact times, we attributed the selectivity drop to the reoxidation of the catalyst bed, which is in excellent agreement with the present results of the activity measurements and the *in situ* HTXRD at low oxygen conversion levels.

As a result of the combustion reaction, the methane-to-oxygen ratio increases at increasing oxygen conversion levels. Figure 3 shows the increase in the CH_4/O_2 ratio in the product gas as a function of the oxygen conversion level during the oxidation of methane over the unreduced catalyst NL. Note the pronounced increase in the methane/oxygen ratio above an oxygen conversion level of 80%. Low methane-to-oxygen ratios clearly favor the formation of nickel oxide. The probability of bulk nickel oxide formation can be expected to decrease at increasing axial position of the nickel crystallites in the catalyst bed due to the increasing methane-to-oxygen ratio in the gas phase. Figure 2 demonstrates that at an oxygen conversion level of 60%, indeed only metallic nickel is observed by means of *in situ* HTXRD. The absence of the nucleation of bulk nickel oxide at high oxygen conversion levels is evident.

Because of the importance for catalysis of information about the surface of the working catalyst, we conducted semi-*in situ* XPS at high oxygen conversion levels, viz., 60 and 85%, corresponding to methane/oxygen ratios of about 4.25 and 8, respectively. For the present investigations we employed a $Ni/SiO_2/Si$ wafer as a nonporous model catalyst with an infinitesimally low activity. Hence, the thus obtained catalytic system can be considered as an extremely differential reactor.

To assess the influence of the oxygen conversion level on the extent of oxidation of the nickel surface layers, we stabilized the previously reduced $Ni/SiO_2/Si$ wafer under reaction conditions. Figure 4 shows the Ni $2p_{1/2}$ and O 1*s* X-ray photoelectron spectra of the thus treated, the reduced, and the reoxidized $Ni/SiO_2/Si$ wafer, respectively. The vertical lines at 852.5 and 868.8 eV in Fig. 4A indicate the positions of the peaks related to metallic nickel, whereas the lines at 854.5 and 872.7 eV indicate the positions of the peaks related to nickel(II). We associate the peak at about 532.3 eV in Fig. 4B with the presence of oxygen in the silica layer on top of the silicon wafer substrate, since it is observed with both the reduced and the oxidized samples. In contrast, the peak at about 529.3 eV is observed only with the oxidized sample. Hence, we associate the latter peak with oxygen present in nickel oxide.

At an oxygen conversion of 60% the Ni $2p_{1/2}$ spectrum clearly displays the presence of nickel oxide, whereas the O 1*s* spectrum most resembles the spectrum of the reduced nickel sample. Note that the O 1*s* electrons have a higher kinetic energy than the Ni $2p_{1/2}$ electrons. The mean free path of the O 1*s* electron is 12 Å, whereas that of the Ni $2p_{1/2}$ electrons is 8 Å. Hence, the O 1*s* signal reflects a thicker (surface) layer than the Ni $2p_{1/2}$ signal. Figure 4A, moreover, shows that an increase in the methane-to-oxygen ratio from about 4.25 to about 8 results in the pronounced contribution

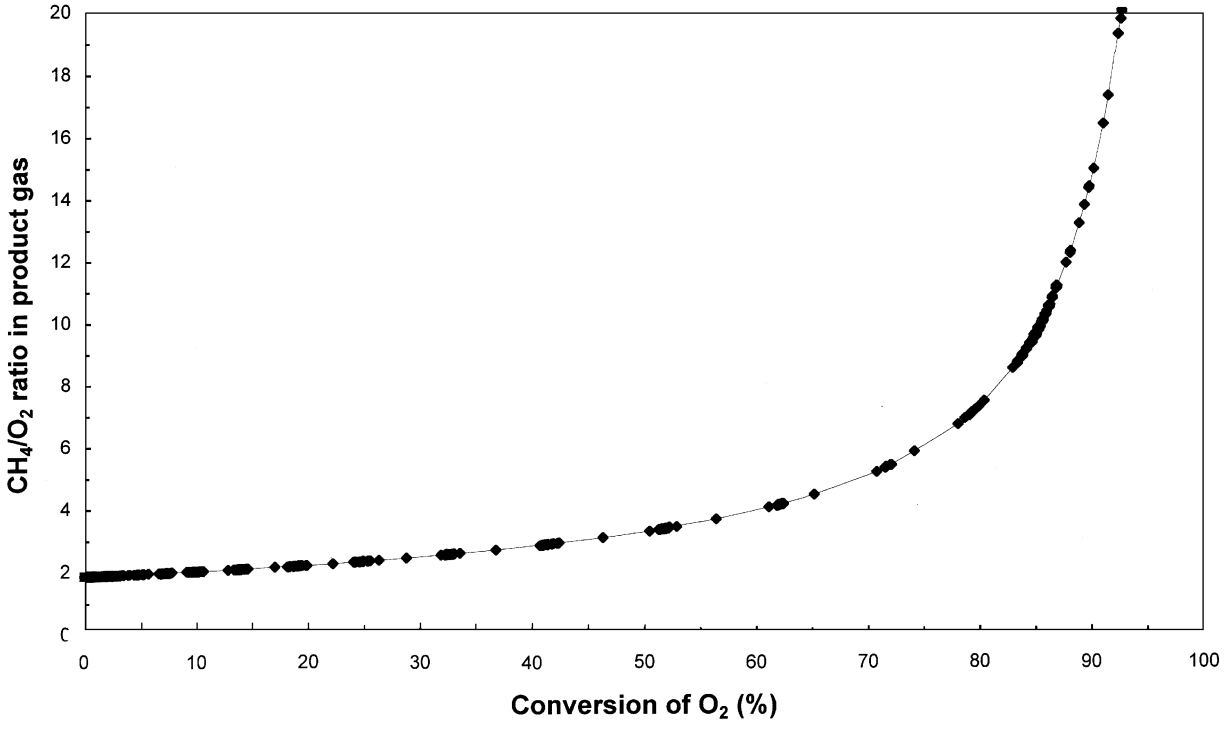

FIG. 3. Methane-to-oxygen ratio in the product gas as a function of the oxygen conversion level during the conversion of methane with oxygen over the unreduced catalyst NL measured at decreasing temperatures.

of metallic nickel along with some oxidic nickel. The difference in the composition of the surface layers obtained at methane-to-oxygen ratios of about 4.25 and 8 is clear.

It should be noted that the XPS results thus obtained are associated with the least reducing conditions plausible under reaction conditions in the catalyst bed: a stronger reducing gas mixture may be present in the catalyst bed than simulated in the current study if the formation of synthesis gas from carbon dioxide, water, and methane occurs along with part of the combustion reaction. We demonstrated that the parallel reforming and combustion of methane can be excluded for oxygen conversions up to at least 25%, since the formation of synthesis gas calls for the presence of metallic nickel sites. At an oxygen conversion level above 25%, however, the bulk of the nickel may be in the zero-valent state, and synthesis gas formation may occur. Hence, the nickel surface could be slightly more reduced than suggested by the present XPS results under reaction conditions in the catalyst bed. In addition, the oxidation of small metal crystallites may proceed at a higher rate than the oxidation of large particles (52). Separately conducted atomic force microscopy (AFM) experiments showed that the height of the nickel crystallites on the wafer was rather small, viz., about 3 to 5 nm. The surface of larger nickel crystallites can be expected to be somewhat less oxidized when employing the same methane-to-oxygen ratio. Unfortunately, a poor signal-to-noise ratio with XPS measurements on a wafer containing nickel crystallites of a size representative for sample NL, viz., about 30 nm, rendered proper analysis of the XPS spectrum difficult. The current XPS results, however, clearly illustrate that the propensity of the gas mixture to reoxidize the nickel surface layers sharply decreases at increasing methane-to-oxygen ratios.

We found that the nature of the nickel phase controlled both the level of conversion of methane and the composition of the mixture of the thus formed product molecules with both the oxidation and reforming of methane, employing either a fully oxidized or a freshly reduced catalyst. Partially oxidized surface layers were found at high oxygen conversion levels by means of semi-*in situ* XPS. It is interesting to compare the partially oxidized nickel crystallites with a fully oxidized sample in terms of their reactivity with respect to methane by means of TPSR experiments. Partially oxidized samples were obtained by carefully oxidizing a freshly reduced catalyst by means of nitrous oxide. Nitrous oxide was employed as an oxidant, since nitrous oxide, in contrast to molecular oxygen, brings about the uniform surface oxidation of the nickel crystallites throughout the catalyst bodies (53). Adjustment of the temperature controls the extent of metal oxidation. The sample thus oxidized was investigated by means of TPSR in a diluted methane stream. The onset temperature of the surface reaction was defined as the temperature at which the consumption of methane started. In all cases, the onset of the conversion of methane

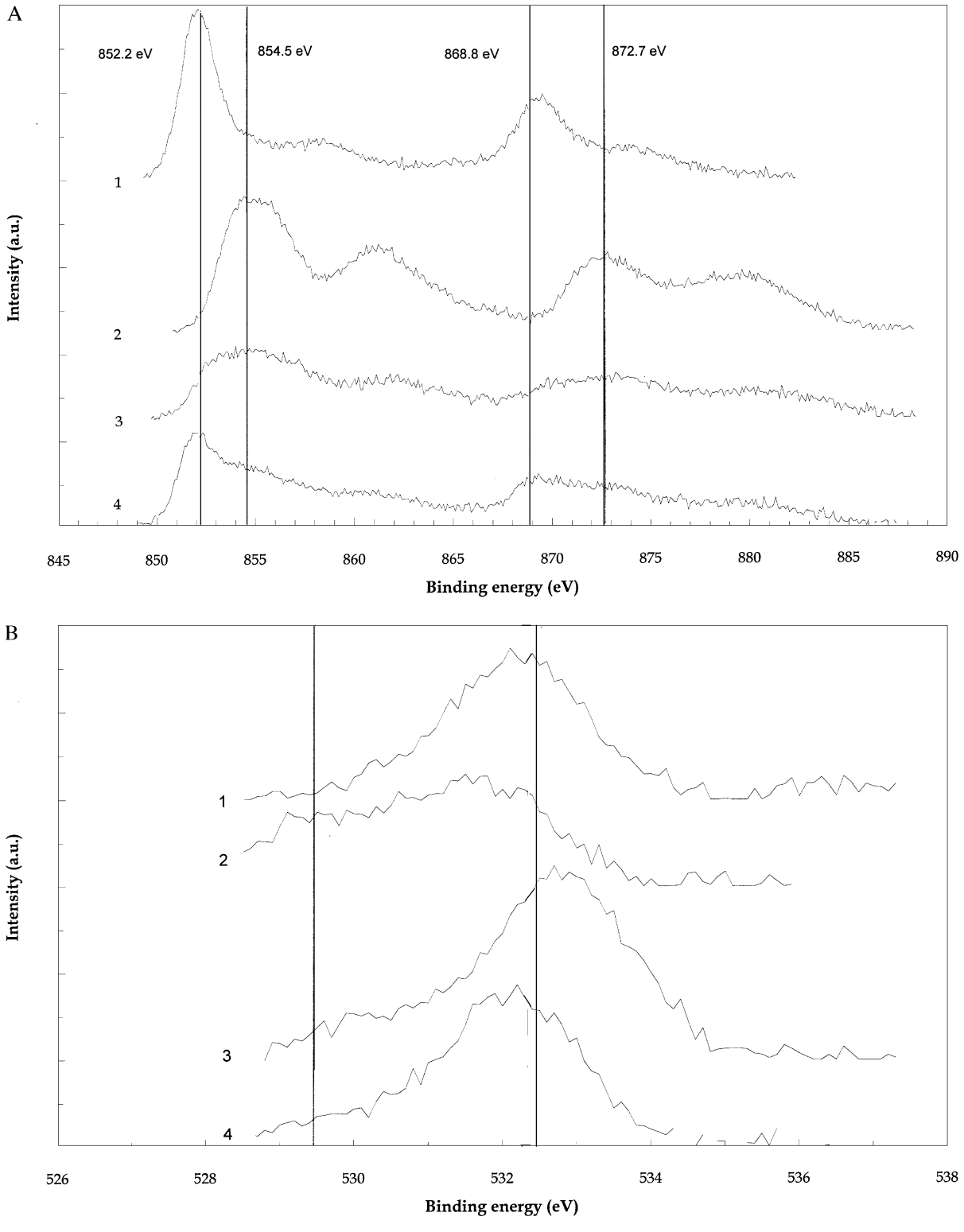

FIG. 4. (A) Ni $2p_{1/2}$ XPS spectrum of $NiO/SiO_2/Si$ wafer subsequent to (1) reduction; (2) reoxidation in a stream of pure oxygen at 720 K for 2 h; and exposure to a gas mixture corresponding to O_2 conversions of (3) 60% and (4) 85%. (B) O 1*s* XPS spectrum of $NiO/SiO_2/Si$ wafer subsequent to (1) reduction; (2) reoxidation in a stream of pure oxygen at 720 K for 2 h; and exposure to a gas mixture corresponding to O_2 conversions of (3) 60% and (4) 85%. For more details refer to the text.

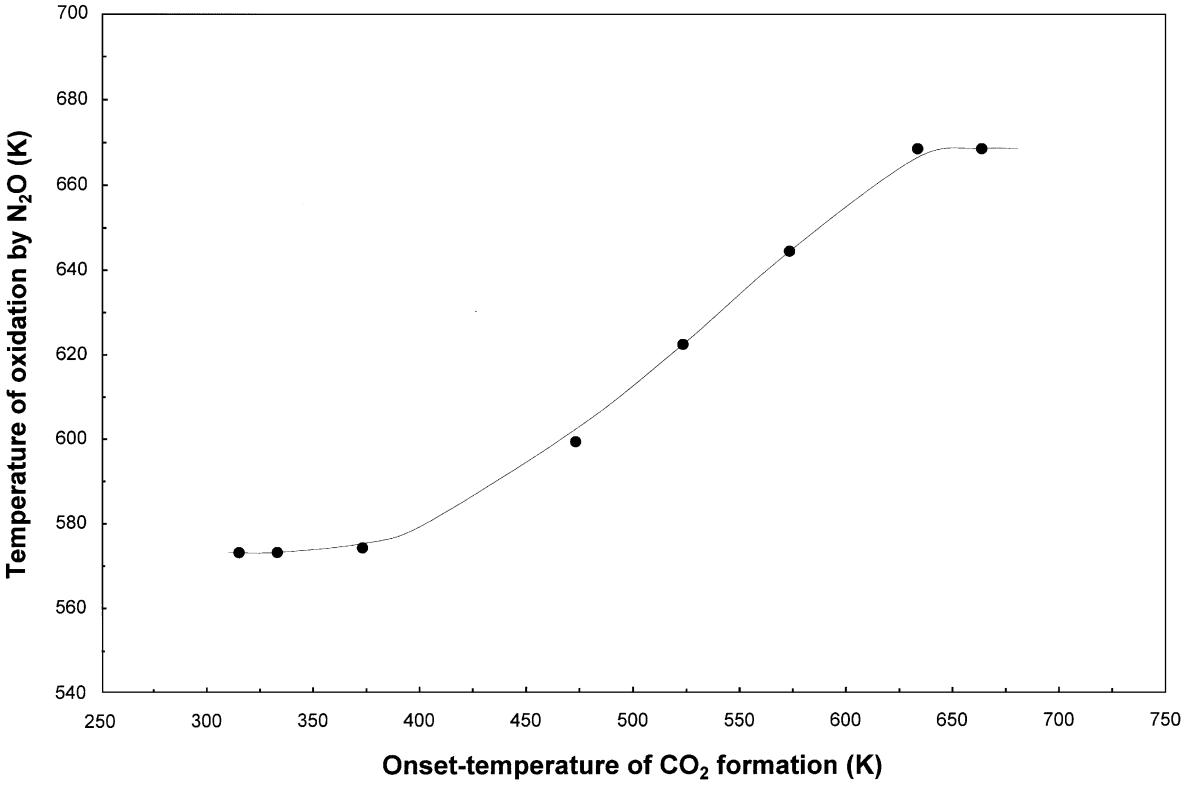

FIG. 5. Onset temperature of the reaction of methane with oxygen from the catalyst under the simultaneous formation of carbon dioxide (and water) as a function of the oxidation temperature of the reduced sample by nitrous oxide. The curve serves only to guide the eye.

coincided with the formation of carbon dioxide (and water vapor). Figure 5 shows the onset temperature of the reaction of methane with oxygen from the catalyst as a function of the temperature at which the oxidation by nitrous oxide has been performed. In addition, the onset temperature of TPSR with a fully oxidized sample is indicated in Fig. 5.

Figure 5 shows that the two-dimensional oxide of a thickness of a few NiO layers, as produced by exposure of a reduced sample to N_2O at about room temperature, reacts with methane already at 573 K. The samples reoxidized at high temperatures, viz., about 630 K, do not react with methane below about 670 K, with this resembling the reactivity of the fully oxidized catalyst. Analogously to catalyst NL, the reactivity of the partially oxidized catalyst NS increases with decreasing extent of nickel oxidation. A superior activity of partially oxidized nickel compared with fully oxidized crystallites agrees with the observations of several workers active in the field of oxidation catalysis. Kalinkin *et al.* (44) rationalized a maximum in the activity of Ni(111) for the oxidation of CO under oxygen-deficient conditions in terms of the optimum activity of a two-dimensional surface oxide compared with the activity of both a fully oxidized and fully reduced nickel surface as supported by their low-energy electron diffraction (LEED) experiments. Moreover, considerably higher reaction probabilities of methane were observed on a passively oxidized Ni(100) surface than for NiO powder in the combustion of methane at atmospheric pressure (54, 55). On the basis of the similarity of the activation energies for the NiO film and for the clean Ni(100) surface, Campbell *et al*. attributed the activation of methane to metallic sites on the NiO film (54). More recently, Burch and Loader (56) investigated the oxidation of methane on platinum under transient conditions. These authors concluded that a partially oxidized platinum surface displays optimum activity compared with a fully reduced or a fully oxidized platinum surface.

The combined body of results demonstrates that the nickel phase in nonuniform along the catalyst bed during the partial oxidation of methane to synthesis gas. At least 25% of the oxygen is converted over bulk nickel oxide to carbon dioxide and water. At high oxygen conversion levels, viz., 60%, the nickel crystallites remain in the reduced state, while the surface seems to be partially oxidized. Finally, the reforming of methane proceeds over metallic nickel sites. The results thus obtained are valuable in contributing to a better understanding of the processes involved in the partial oxidation of methane to synthesis gas. Analogously to other investigations (21, 25), the activity of catalyst NL as a function of the temperature in the catalyst bed exhibits a hysteresis (see Fig. 6). The

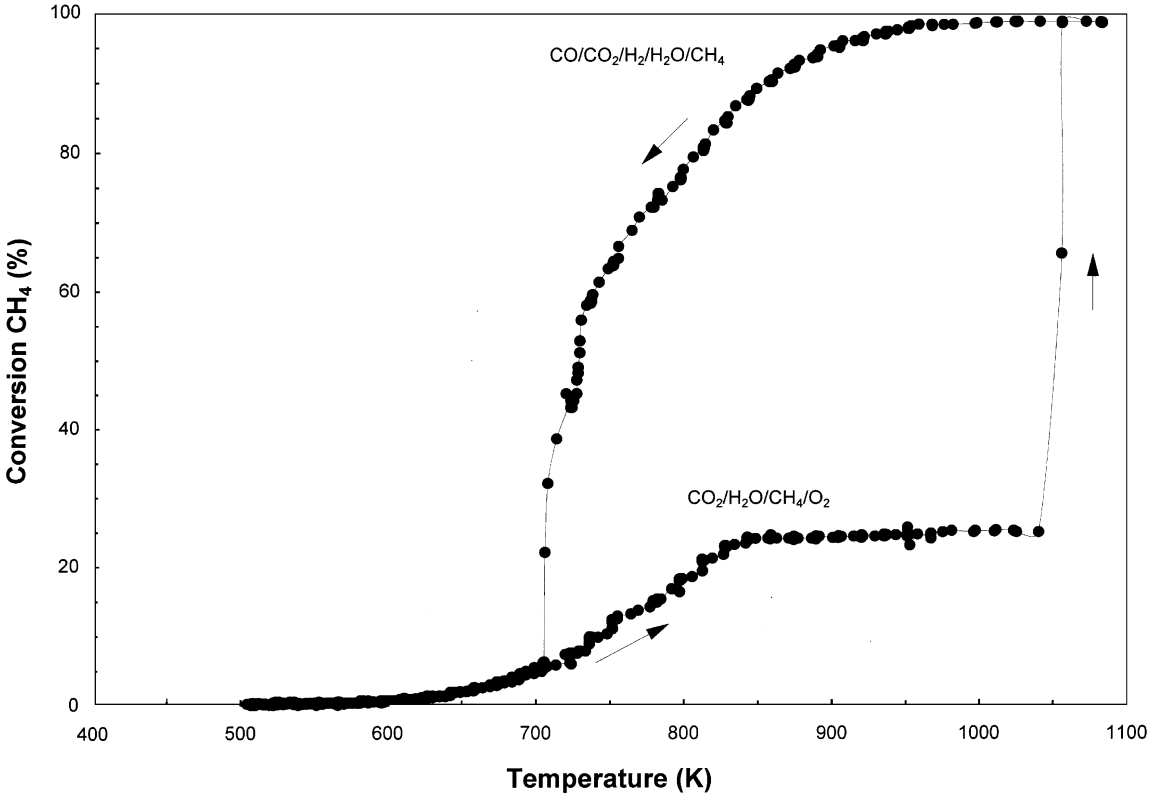

FIG. 6. Conversion of methane as a function of the temperature during the partial oxidation of methane over catalyst NL. The product molecules are indicated in the figure.

unreduced nickel oxide catalyst converts only 20% of the methane at 825 K, while carbon dioxide and water are the only products. At higher temperatures the conversion of methane suddenly sharply increases from about 25% to almost 100%, accompanied by the production of synthesis gas. The oxygen balance, moreover, exceeds 100% for a limited period due to the reduction of the catalyst. The methane conversion level is close to 90% at 825 K, while synthesis gas is the main product. The resemblance of the hysteresis to the separately determined activity curves as depicted in Fig. 1, employing either an unreduced or a freshly reduced sample NL, is clear. From the difference in the methane conversion levels at 825 K, we conclude that a necessary condition for the formation of synthesis gas is the presence of an active phase with a combustion activity considerably higher than that of nickel oxide. We suggest that the enhanced combustion activity under the conditions of synthesis gas formation is related to the presence of a partially oxidized nickel surface. Subsequent to the combustion of methane, the production of synthesis gas by means of the reforming of methane with water vapor and carbon dioxide proceeds over metallic nickel sites.

The presented investigations demonstrate that the atmosphere is oxidizing at zero conversion, but reducing at high conversion. As a consequence, the relative stabilities of nickel metal and oxide depend on the conversion. In addition, the deposition of carbon on the catalyst with the partial oxidation of methane has been reported (57). The simultaneous presence of oxidic, metallic, and carbidic and/or graphitic phases is one of the reasons why the chemistry of the partial oxidation of methane is so complicated.

Finally, we discuss the consequences of the present results for mechanistic studies. Experiments conducted at low oxygen conversion levels exclusively provide information about the reaction mechanism at relatively low methane-to-oxygen ratios. Hence, the elucidation of the mechanism of the partial oxidation of methane in a fixed bed reactor calls for a combination of steady-state measurements conducted at both low and high methane conversion levels. Pulse experiments may also contribute to a better understanding of the reaction mechanism under steady-state conditions provided (58) (i) the composition of the catalytically active phase is uniform along the catalyst bed, (ii) the conversion of the reactants is sufficiently low, and (iii) the composition of the surface is representative of the situation under steady-state conditions. The present study shows that the oxygen conversion level strongly affects the nature of the active phase. Accordingly, the catalyst bed can be expected to be nonuniform in terms of the phase composition if the product gas mixture lacks molecular oxygen. This

renders pulse experiments in which oxygen is completely consumed highly unreliable for the elucidation of the mechanism of the partial oxidation of methane to synthesis gas in fixed bed reactors under steady-state conditions. The same applies to investigations employing fluidized bed reactors, since the position of the catalyst particles is not fixed.

CONCLUSIONS

The combination of *in situ* HTXRD, semi-*in situ* XPS, activity, and TPSR experiments shows that the nature of the active phase of the nickel catalyst significantly varies with the oxygen conversion level. The atmosphere is oxidizing at zero conversion, but reducing at high conversion. At oxygen conversions up to at least 25% the combustion of methane at about 825 K proceeds over nickel oxide. At higher oxygen conversion levels, the bulk of the nickel crystallites remains in the zero-valent state, while the surface is probably oxidized. It is suggested that the partially oxidized nickel crystallites display a higher combustion activity than fully oxidized nickel particles. Finally, the reforming of methane to synthesis gas proceeds over metallic nickel sites.

Summarizing, the composition of the catalyst surface is not uniform along the catalyst bed. This highly complicating factor should be taken into account with the study of the mechanism of the partial oxidation of methane to synthesis gas in a fixed bed reactor. Results of mechanistic studies using either a fluidized bed reactor or a pulse apparatus at high oxygen conversion levels should be considered with care.

ACKNOWLEDGMENTS

We thank Mr. Mens for performing the XPS measurements. The HTXRD experiments by Mrs. Versluijs and highly appreciated. We thank GASTEC for financial support.

REFERENCES

1. Kunz, R. G., Smith, D. D., Patel, N. M., Thompson, G. P., and Patrick, G. S., *Hydrocarbon Process.* **71**, 57 (1992).
2. Baade, W. F., Snyder, G. D., and Abrardo, J. M., *Hydrocarbon Process.* **72**, 77 (1993).
3. Rostrup-Nielsen, J. R., *Catal. Today* **18**, 305 (1993).
4. Solbakken, Å., *in* "Natural Gas Conversion" (A. Holmen, Ed.), p. 447. Elsevier, Amsterdam, 1991.
5. Farina, G. L., and Supp, E., *Hydrocarbon Process.* **71**, 77 (1992).
6. Trimm, D. L., and Wainwright, M. S., *Catal. Today* **6**, 261 (1990).
7. Michel, S., *Hydrocarbon Process.* **68**, 37 (1989).
8. Marsch, H. D., and Herbort, H. J., *Hydrocarbon Process.* **61**, 101 (1982).
9. Christensen, T. S., and Primdahl, I. I., *Hydrocarbon Process.* **73**, 39 (1994).
10. Schneider, R. V., III, and LeBlanc, J. R., *Hydrocarbon Process.* **71**, 51 (1992).
11. Pena, M. A., Gomez, J. P., and Fierro, J. L. G., *Appl. Catal. A* **144**, 7 (1996).
12. Heitnes Hofstad, K., Rokstad, O. A., and Holmen, A., *Catal. Lett.* **36**, 25 (1996).
13. Buyevskaya, O. V., Walter, K., Wolf, D., and Baerns, M., *Catal. Lett.* **38**, 81 (1996).
14. Basini, L., Aragno, A., and Vlaic, G., *Catal. Lett.* **39**, 49 (1996).
15. Boucouvalas, Y., Zhang, Z., and Verykios, X., *Catal. Lett.* **40**, 189 (1996).
16. Boucouvalas, Y., Zhang, Z. I., Efstathiou, A. M., and Verykios, X. E., *in* "Proceedings, 11th International Congress on Catalysis" (J. W. Hightower, W. N. Delgass, E. Iglesia, and A. T. Bell, Eds.), Stud. Surf. Sci. Catal. 101, p. 443. Elsevier, Amsterdam, 1996.
17. Kröger, C., *Z. Anorg. Allg. Chem.* **206**, 289 (1932).
18. Prettre, M., Eichner, C., and Perrin, M., *Trans. Faraday Soc.* **42**, 335 (1946).
19. Huszár, K., Rácz, Gy., and Székely, Gy., *Acta Chim. Acad. Sci. Hung.* **70**, 287 (1971).
20. Vernon, P. D. F., Green, M. L. H., Cheetham, A. K., and Ashcroft, A. T., *Catal. Lett.* **6**, 181 (1990).
21. Dissanayake, D., Rosynek, M. P., Kharas, K. C. C., and Lunsford, J. H., *J. Catal.* **132**, 117 (1991).
22. Witt, P. M., and Schmidt, L. D., *J. Catal.* **163**, 465 (1996).
23. Chang, Y.-F., and Heinemann, H., *Catal. Lett.* **21**, 215 (1993).
24. Choudhary, V. R., Rajput, A. M., and Prabhakar, B., *J. Catal.* **139**, 326 (1993).
25. Van Looij, F., Van Giezen, J. C., Stobbe, E. R., and Geus, J. W., *Catal. Today* **21**, 495 (1994).
26. Hayakawa, T., Andersen, A. G., Shimizu, M., Suzuki, K., and Takehira, K., *Catal. Lett.* **22**, 307 (1993).
27. Torniainen, P. M., Chu, X., and Schmidt, L. D., *J. Catal.* **146**, 1 (1994).
28. Slagtern, Å., and Olsbye, U., *Appl. Catal. A* **110**, 99 (1994).
29. Au, C. T., Hu, Y. H., and Wan, H. L., *Catal. Lett.* **27**, 199 (1994).
30. Dell, R. M., and Stone, F. S., *Trans. Faraday Soc.* **50**, 501 (1954).
31. Boreskov, G. K., *in* "Catalysis Science and Technology" (J. R. Anderson and M. Boudart, Eds.), Vol. 3, p. 39. Springer-Verlag, Berlin/New York, 1982.
32. Savchenko, V. I., *Kinet. Catal.* **31**, 624 (1990).
33. Roberts, M. W., *Surf. Sci.* **299/300**, 769 (1994).
34. De Bokx, P. K., Labohm, F., Gijzeman, O. L. J., Bootsma, G. A., and Geus, J. W., *Appl. Surf. Sci.* **5**, 321 (1980).
35. Norton, P. R., Tapping, R. L., and Goodale, J. W., *Surf. Sci.* **65**, 13 (1977).
36. Al-Sarraf, N., Stuckless, J. T., Wartnaby, C. E., and King, D. A., *Surf. Sci.* **283**, 427 (1993).
37. Trapnell, B. M. W., *in* "Chemisorption" (W. E. Garner, Ed.), p. 100. Butterworth, Stoneham, MA, 1957.
38. Dell, R. M., Klemperer, D. F., and Stone, F. S., *J. Phys. Chem.* **60**, 1586 (1956).
39. Benziger, J. B., *Appl. Surf. Sci.* **6**, 105 (1980).
40. Toyoshima, I., and Somorjai, G. A., *Catal. Rev. Sci. Eng.* **19**, 105 (1979).
41. Nieuwenhuys, B. E., *Surf. Sci.* **126**, 307 (1983).
42. Brennan, D., Hayward, D. O., and Trapnell, M. W., *Proc. R. Soc. A* **256**, 81 (1960), and references therein.
43. Norton, P. R., and Tapping, R. L., *Faraday Disc. Chem. Soc.* **60**, 71 (1975).
44. Kalinkin, A. V., Boreskov, G. K., Savchenko, V. I., and Dadayan, K. A., *React. Kinet. Catal. Lett.* **13**, 111 (1980).
45. Benninghoven, A., Beckmann, P., Muller, K. H., and Schemmer, M., *Surf. Sci.* **89**, 701 (1979).
46. Golodets, G. I., *in* "Heterogeneous Catalytic Reactions Involving Molecular Oxygen" (J. R. H. Ross, Ed.), Stud. Surf. Sci. Catal. 15, p. 45. Elsevier, Amsterdam, 1983.
47. Hermans, L. A., and Geus, J. W., *in* "Scientific Bases for the Preparation of Heterogeneous Catalysts" (B. Delmon, P. Grange, P. Jacobs, and G. Poncelet, Eds.), Vol. B2, p. 1. Elsevier, Amsterdam, 1979.

48. Van Wijk, R., Gijzeman, O. L. J., Geus, J. W., Ten Grotenhuis, E., and Van Miltenburg, J. C., *Catal. Lett.* **24**, 171 (1994).
49. Kuipers, E. W., Laszlo, C., and Wieldraaijer, W., *Catal. Lett.* **17**, 71 (1993).
50. Ten Grotenhuis, E., Van Miltenburg, J. C., Van der Eerden, J. P., Van Wijk, R., Gijzeman, O. L. J., Geus, J. W., and Marée, C. H. M., *Catal. Lett.* **28**, 109 (1994).
51. Van de Kleut, D., Ph.D. thesis, Utrecht University, Utrecht, 1994.
52. Manogue, W. H., and Katzer, J. R., *J. Catal.* **32**, 166 (1974).
53. Kuijpers, E. G. M., Ph.D. thesis, Utrecht University, Utrecht, 1982.
54. Campbell, R. A., Szanyi, J., Lenz, P., and Goodman, D. W., *Catal. Lett.* **17**, 39 (1993).
55. Hall, R. B., Chen, J. G., Hardenbergh, J. H., and Mims, C. A., *Langmuir* **7**, 2548 (1991).
56. Burch, R., and Loader, P. K., *Appl. Catal. A* **122**, 169 (1995).
57. Claridge, J. B., Green, M. L. H., Chi Tsang, S., York, A. P. E., Ashcroft, A. T., and Battle, P. D., *Catal. Lett.* **22**, 299 (1993).
58. Frennet, A., *in* "Elementary Reaction Steps in Heterogeneous Catalysis" (R. W. Joyner and R. A. van Santen, Eds.), p. 423. Kluwer Academic, Dordrecht/Norwell, MA, 1993.